

Gradient enhancement of the total magnetic field

STEPHEN REFORD, Paterson, Grant & Watson Limited, Toronto, Canada

The collection of magnetic gradiometer data using a configuration of two, three, or four magnetometers has become commonplace. One use of these data is to improve the accuracy and resolution of the gridded total magnetic field beyond what can be interpolated from a single magnetometer. This is especially important for anomalies over small magnetic sources that lie between survey lines and over linear sources that strike obliquely to the survey lines. As an alternative to improved accuracy and resolution, one can consider increasing the survey line spacing to obtain the equivalent total magnetic field, thereby reducing the survey cost.

Gridding methods. The improved resolution and accuracy of the measured horizontal gradients, over the corresponding derivatives computed from total magnetic field, are clearly demonstrated in McMullan and McLellan (1997). Therefore, it is sensible to incorporate the measured gradients when interpolating the total magnetic field. The lateral gradient (i.e., the horizontal gradient perpendicular to the survey line direction) is the most critical because it provides the most information regarding the behavior of the magnetic field in the gaps between the survey lines.

The gradient tensor method to compute the gradient-enhanced total magnetic field, incorporating the measured total magnetic field and the two measured horizontal gradients (lateral or across-line, and longitudinal or along-line), is briefly described by Hogg (2004), and compared to other methods with favorable results. The technical details of the technique are not given, so it is not possible to implement the method for inclusion in this comparison.

This paper evaluates two conventional gridding techniques applied to aeromagnetic data, and two gradient-enhanced techniques. All are available as part of a widely used commercial software package (OASIS montaj from Geosoft). The conventional techniques are:

- Bidirectional gridding, which applies a spline (linear, Akima or cubic) along the survey lines and then across the survey lines
- Minimum curvature gridding, which fits the data to a constrained minimum curvature surface (Smith and Wessel, 1990)

The first gradient enhancement technique is described in Nelson (1994). The gridded total magnetic field is derived in the Fourier domain from the leveled and gridded lateral and longitudinal gradients, using the generalized 3D Hilbert transform relations. It was implemented by Nelson as a method of producing a leveled total magnetic field without the need of conventional tie-line leveling. This assumes that the total field level errors are due to diurnal variation. The measured gradients are minimally affected by diurnal. The problem with this approach is that the longest wavelengths in the total magnetic field generally produce small gradients, with amplitudes below the noise levels of a typical survey. Our approach is to level the gradients and use them to compute a “pseudo” total magnetic field. We also grid the leveled total magnetic field and use it to apply a long wave-

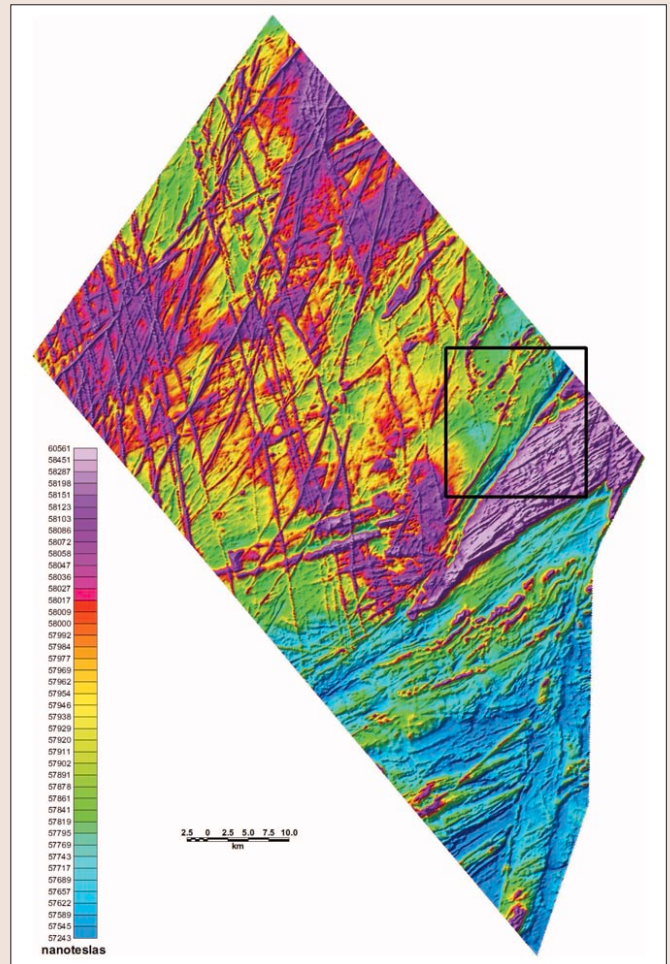


Figure 1. Total magnetic field image of the study area, prepared using bidirectional gridding (subset area used in later figures outlined in black).

length correction to the “pseudo” total magnetic field.

The second gradient enhancement technique is described in Hardwick (1999). It uses the measured lateral gradient from two wingtip-mounted sensors to extrapolate values of the total magnetic field onto “pseudolines” at a specified distance on either side of the survey line. These values are then included in the interpolation of the total magnetic field.

To test the gridding techniques, standard data processing was applied. Extensive effort to prepare the best possible product was not undertaken, as it would not simulate a production situation, and might hide some of the issues associated with each method.

Study area. A 105 848-line-km aeromagnetic survey was flown over the Kapuskasing Structural Zone in northeastern Ontario using three different contractors (GSC, 2001). The geology of the survey area was described as follows:

The eastern extent of the survey area covers a portion of the Kapuskasing Structural Zone (KSZ) and covers a large area west of this structure. The KSZ represents an oblique cross section exposing about 20 km of upper and middle Archean crust uplifted along an east-verging thrust fault in the central part of the Superior Province. In the south, it grades from greenschist facies supracrustal rocks

Editor's note: All grids utilized in the preparation of this paper may be obtained by contacting the author.

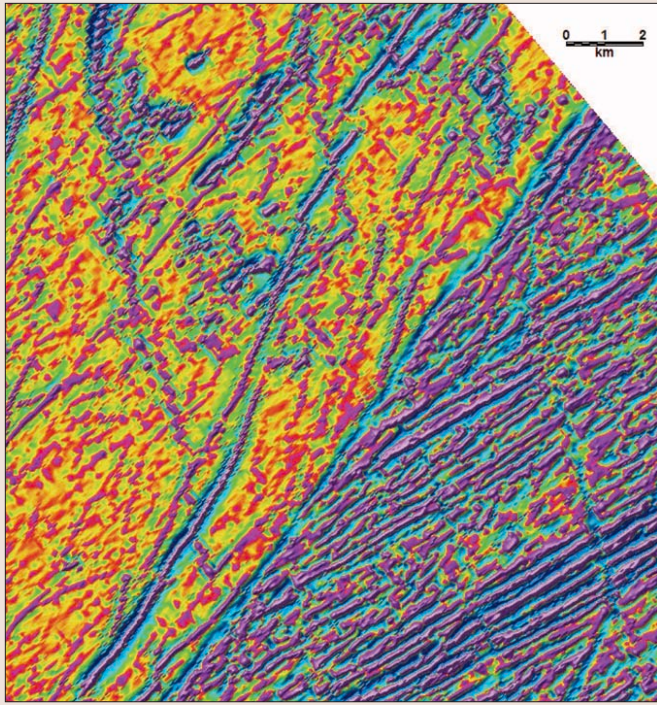


Figure 2. Enhanced residual image computed from the total magnetic field for a portion of the study area, prepared using bidirectional gridding.

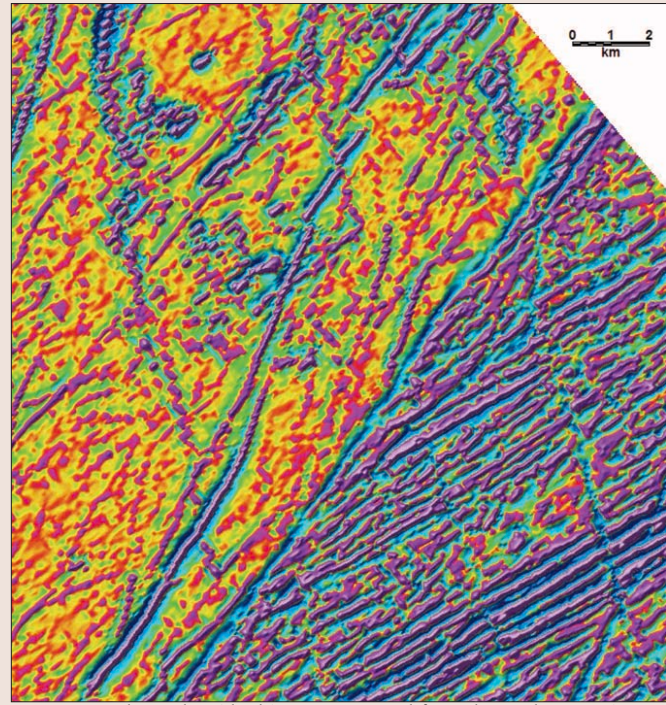


Figure 3. Enhanced residual image computed from the total magnetic field for a portion of the study area, prepared using bidirectional gridding and smoothed.

and granitic rocks of the Wawa Subprovince in the west to granulite facies gneisses representing the deepest part of the section, truncated against greenstone and granitic rocks of the Abitibi Subprovince in the east.

Further to the north, metasedimentary rocks of the Quetico Subprovince are uplifted and truncated against granitic rocks of the Opatica Subprovince. As the zone was the locus of major uplift of Archean crust and upper mantle, it has excellent potential for mineral deposits within rocks units that have tapped these deep seated sources such as diamonds in kimberlites and lamprophyres, and phosphates and rare earth metals in carbonates. In addition, there may be good potential for PGEs, base metals and industrial minerals in mafic intrusions, anorthosite bodies such as the Shawmere complex and within greenstone enclaves.

The surficial cover over most of the survey area is thin. Thicker accumulations of up to tens of meters of till and glaciolacustrine deposits occur in the northern portion of the survey area.

The survey lines were flown 200 m apart at 320° azimuth, and at a nominal terrain clearance of 100 m. The control lines were flown 1600 m apart at 50° azimuth. The 10-Hz sampling results in magnetic values measured every 8 m or so along the lines. One of the contractors, Goldak Airborne Surveys, employed a three-magnetometer configuration (two wingtip sensors mounted 14.8 m apart, and a tail stinger situated 9.8 m to the rear). The survey was contracted for a single sensor, so the magnetic data from the wingtip magnetometers were compensated and lag-corrected, but no further compilation was undertaken. The data from the tail magnetometer were subjected to standard leveling procedures.

Results of conventional gridding. All grids were prepared at a 25-m grid cell interval (i.e., one-eighth the line spacing). Some may consider this a small interval, but it provides a better depiction of the spatial resolution with and without gradient enhancement, and also shows high-frequency noise and aliasing associated with the gridding techniques.

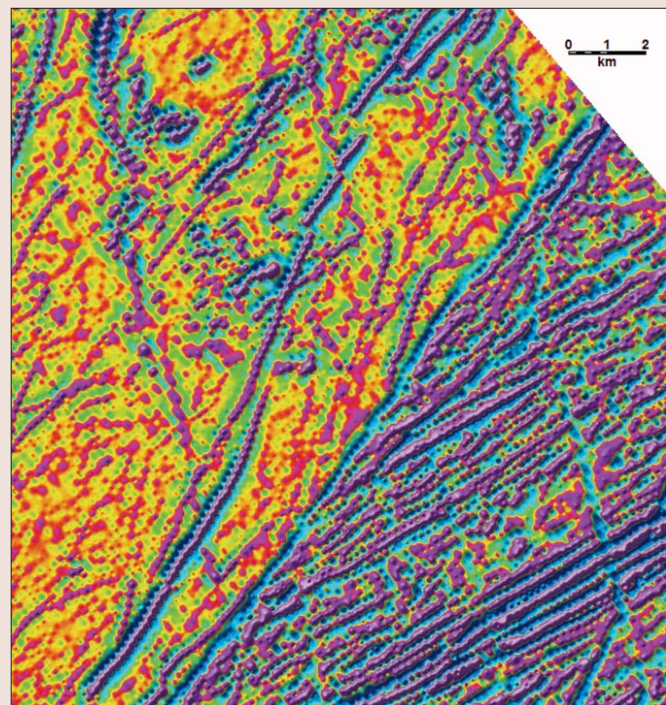


Figure 4. Enhanced residual image computed from the total magnetic field for a portion of the study area, prepared using minimum curvature gridding.

Aliasing occurs due to the difference in sampling in the line direction (8 m) compared to the sampling perpendicular to the line direction (200 m). It may appear as “beading” along linear anomalies, stretching of anomalies in the wrong direction or distorted anomaly shapes, particularly where the anomaly strike is at a low angle relative to the line direction. Wherever smoothing has been applied, it consisted of two passes of a 3×3 space-domain Hanning filter. All shading is from the northwest, in the flightline direction.

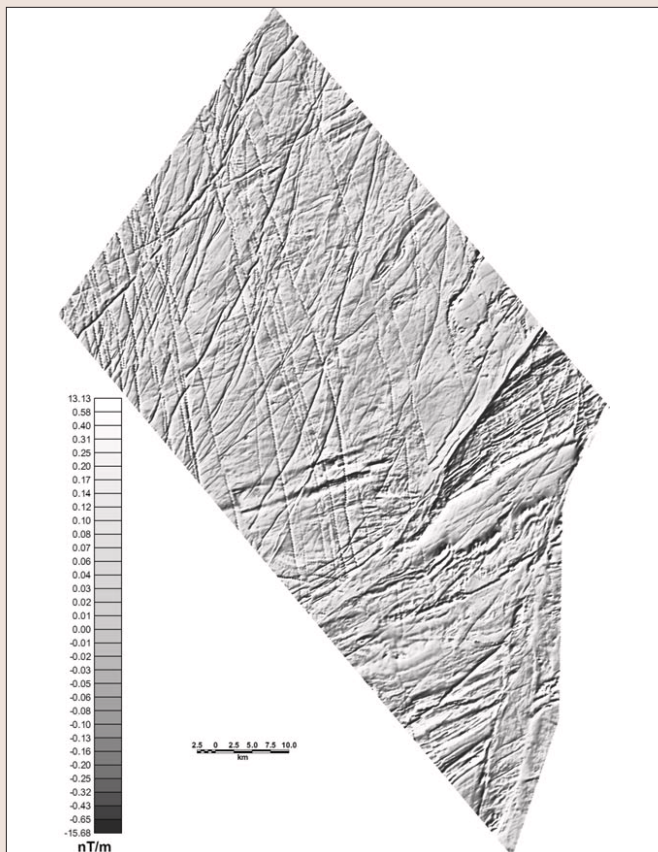


Figure 5. Longitudinal gradient image of the study area computed by time differencing, prepared using bidirectional gridding.



Figure 6. Lateral gradient image of the study area computed by spatial differencing, prepared using bidirectional gridding.

The enhanced residual is used as a high-frequency enhancement to examine the detail in the various grids. It is computed by applying two passes of a Hanning 3×3 smoothing filter to the total magnetic field grid, and then subtracting the smoothed grid from the original. Qualitatively, it is quite similar to a second vertical derivative and is useful for examining short-wavelength anomalies and high-frequency noise.

Figure 1 shows the total magnetic field interpolated using bidirectional gridding. Since the survey lines are not oriented along a Cartesian grid axis, the gridding was applied in two stages:

- 1) The data are interpolated at a 25-m interval using an Akima spline, first along the flightline, and then perpendicular to the line direction, resulting in a grid rotated in the line direction.
- 2) The grid is regridded to reorient the grid to the Cartesian coordinate system.

Figures 2 and 3 show the unsmoothed and smoothed versions of the enhanced residual, respectively. As anticipated, this gridding method works well for anomalies striking nearly perpendicular to the line direction but shows significant aliasing for those striking at more oblique angles. Also, a tearing effect of the regridding process is evident but greatly diminished by smoothing.

Figure 4 shows the enhanced residual of the total magnetic field interpolated using minimum curvature gridding. It shows the typical "spottiness" for all strike directions but renders the oblique angle linear anomalies somewhat more faithfully.

Gradient processing. The largest contiguous block of gradiometer data is located in the northern part of the survey area. We processed 20 658 line-km of traverse line data, computing and leveling the lateral and longitudinal gradients. We used two methods to compute the longitudinal gradient. One method was to difference the mean of the two wingtip total magnetic field measurements with that of the tail measurement, and divide by the distance. The second was to compute the time derivative between successive measurements of the tail stinger and divide by the instantaneous velocity. The first approach is free of diurnal activity but will incorporate level differences between the three sensors, and will magnify independent sources of noise. The second does not suffer from leveling issues but is susceptible to noise from geomagnetic micropulsations. For this survey, the longitudinal gradient using the time-derivative of the tail stinger proved more reliable, due to the low noise and lack of level errors. The longitudinal gradient grid prepared using bidirectional gridding is shown in Figure 5.

The lateral gradient was computed by differencing the two wingtip total magnetic field measurements and dividing by the sensor separation. It contained block level shifts, which were removed using a second-order polynomial. It then required microleveling. Some residual line noise remains at a few locations, which can be removed using more careful treatment. A fairly significant level bust extending from the southeast edge of the survey could not be fully removed by microleveling. The lateral gradient grid prepared using bidirectional gridding is shown in Figure 6.

Results of gradient-enhanced gridding. The enhanced residual of the gradient-enhanced total magnetic field computed using the Hardwick method is shown in Figure 7. The Hardwick method was computed using bidirectional grid-

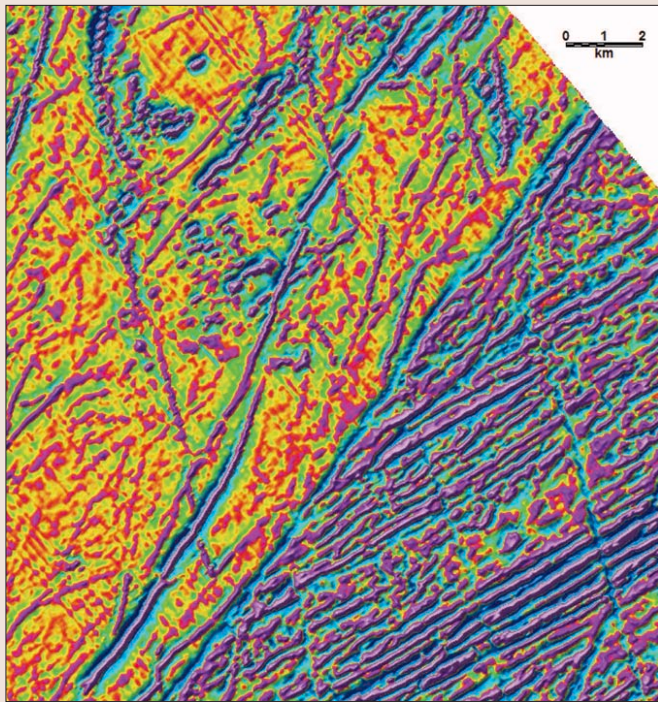


Figure 7. Enhanced residual image computed from the gradient-enhanced total magnetic field for a portion of the study area, prepared using Hardwick's method with bidirectional gridding and smoothed.

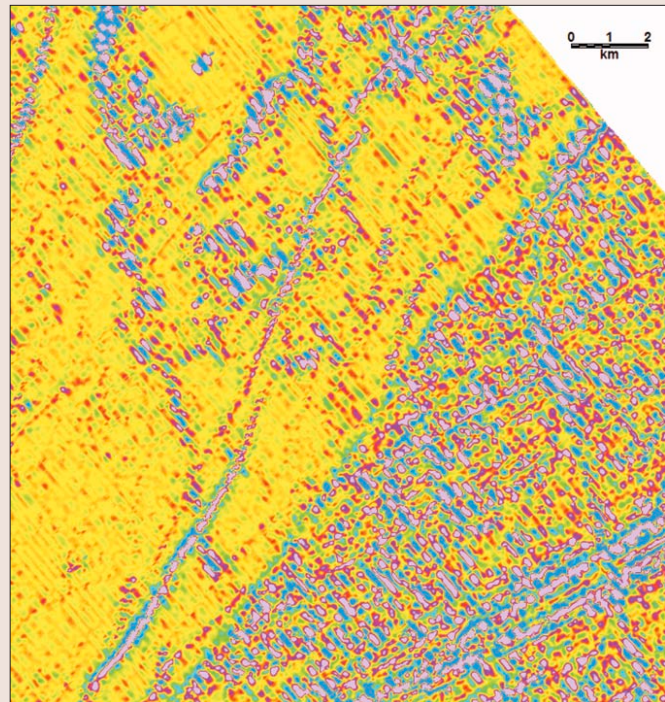


Figure 8. Image of the difference between the total magnetic field (Figure 1) and gradient-enhanced total magnetic field computed using Hardwick's method (Figure 7), linearly scaled between -5 nT and 5 nT.

ding only, as it is incorporated in that gridding module. Figure 8 shows the difference between the total magnetic field grids computed using standard bidirectional gridding and the Hardwick method. Smoothing was applied to diminish the tearing effect of the bidirectional gridding. The continuity of the linear anomalies is significantly improved, and the nonlinear anomalies show a more realistic curvature. The method has introduced level noise in some low-gradient areas. There is a parameter that can adjust the noise threshold, which affects how the measured lateral gradient is blended with the lateral gradient computed from the gridded total magnetic field. Raising this threshold would reduce the level noise but also reduce the effectiveness of the gradient enhancement. Since the problem appears to be restricted to certain lines only, more careful leveling of the lateral gradient channel prior to gridding would minimize the problem. The difference grid shows where the method has had an effect on the gridding, consisting of sharp lateral changes between adjacent survey lines over the peaks and flanks of anomalies. It also shows that the smoothing process has clipped anomaly peaks. Bear in mind that the Hardwick method uses the lateral gradient only.

Figure 9 shows the enhanced residual of total magnetic field computed using the Nelson method, from the lateral and longitudinal gradient grids prepared using bidirectional gridding. The Nelson method uses the gradients only to reconstruct the total magnetic field and cannot properly recover the regional component. This was corrected by adding a low-pass filtered version of the measured total magnetic field to a high-pass filtered version of the Nelson "pseudo" total magnetic field. An eighth-order Butterworth filter with 400-m cutoff wavelength (i.e., twice the flightline spacing) was employed in both cases. Comparison of the enhanced residuals before and after the regional correction shows that the shortest wavelengths are not affected by the correction. Computing the difference between the measured and reconstructed total magnetic field (Figure 10) confirms that the long wavelengths are preserved. The choice of the

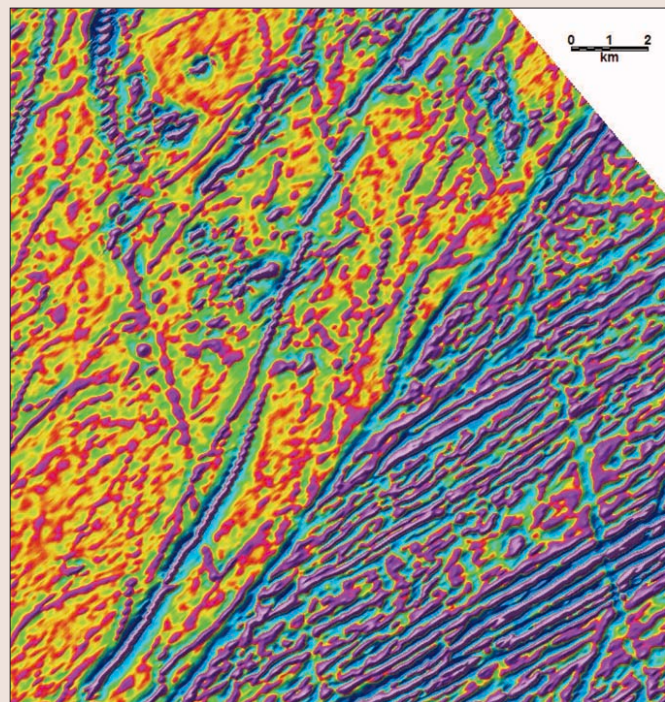


Figure 9. Enhanced residual image computed from the gradient-enhanced total magnetic field for a portion of the study area, prepared using Nelson's method and bidirectional gridding.

regional correction does affect the intermediate wavelengths (e.g., a 1000-m cutoff wavelength rather than 400 m results in a smoother total magnetic field, clipping the anomaly peaks). Some overshoot on the flanks of sharp anomalies is evident.

Figure 11 shows the enhanced residual of the total magnetic field prepared as described above, except that the gradient grids were interpolated using minimum curvature gridding. Since the Nelson method utilizes grids of the gra-

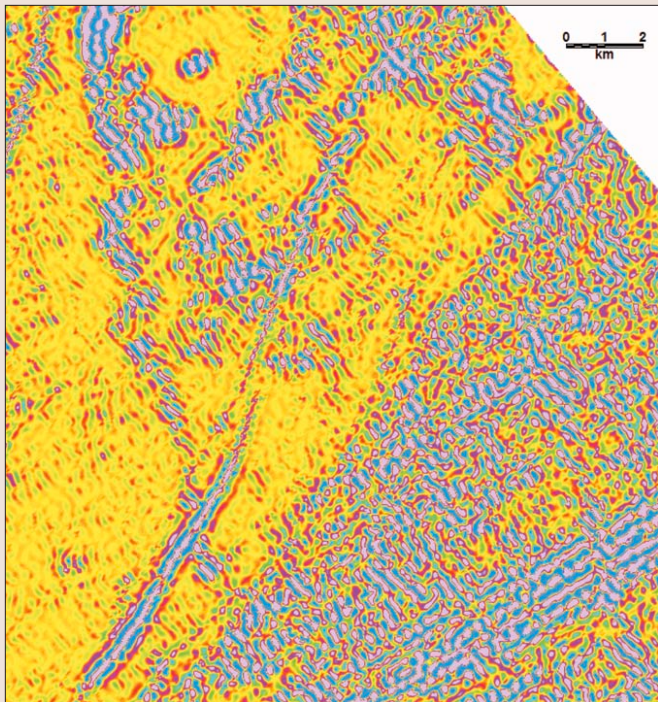


Figure 10. Image of the difference between the total magnetic field (Figure 1) and gradient-enhanced total magnetic field computed using Nelson's method (Figure 9), linearly scaled between -5 nT and 5 nT.

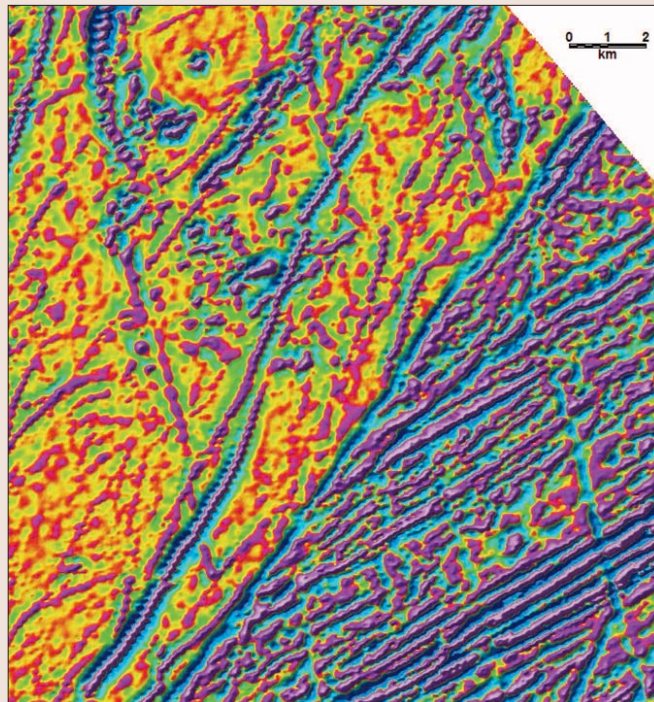


Figure 11. Enhanced residual image computed from the gradient-enhanced total magnetic field for a portion of the study area, prepared using Nelson's method and minimum curvature gridding.

dients, it is dependent on the quality of the gradient grids themselves. Comparison of the Nelson enhanced residuals from bidirectional and minimum curvature gridding (Figures 9 and 11, respectively) shows the aliasing characteristics of these methods described earlier but greatly diminished compared to the grids prepared without gradient enhancement. In comparison to the Hardwick method, the Nelson method shows less continuity of the linear anomalies, especially those with oblique strike direction. The minimum curvature version of the Nelson method is superior in this sense to the bidirectional version. The beading effect is still present in the minimum curvature version.

To improve the grids of the lateral and longitudinal gradients, automated trend enforcement was applied to reinforce the gridding of the linear anomalies. The process is applied to the profile data, searching for positive and negative anomaly peaks on each survey line, joining peaks with similar characteristics, eliminating cross-cutting trends and then interpolating along the trends to add "pseudo-lines" to the profile data. These trends are then included in the interpolation process with the regular survey lines. The displayed trends are a combination of those striking between 20° E and 80° E, with a minimum length of 1500 m, and of those striking between 70° E and 330° W, with a minimum length of 3500 m. The study area is quite challenging for automated trend detection due to the numerous, intersecting anomalies striking in all directions. Those striking sub-parallel to the flightline direction are difficult to detect automatically but could be added manually.

Figure 12 shows the enhanced residual of the total magnetic field, with the addition of trend enforcement prior to minimum curvature gridding, and using the 400 -m cutoff wavelength for the regional correction. Where the trends have been added, the aliasing associated with this type of gridding has been reduced considerably.

Each of the gradient enhancement techniques has its strengths and weaknesses. In these examples, the Hardwick method shows the best continuity of linear features in all

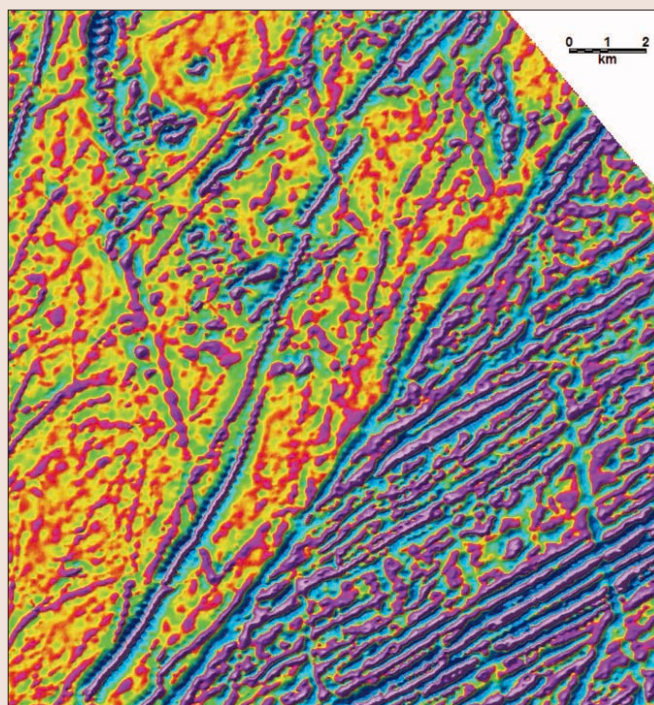


Figure 12. Enhanced residual image computed from the gradient-enhanced total magnetic field for a portion of the study area, prepared using Nelson's method and minimum curvature gridding, with geological trends incorporated.

directions but is also susceptible to residual line noise. It should be possible to eliminate the noise through careful leveling and microleveling. The Nelson method that employed minimum curvature gridding still shows some beading. The Nelson method that employed bidirectional gridding is free of noise but lacks some continuity in the survey line direction. We have improved the Nelson method by incorporating automated detection and interpolation along lin-

ear trends prior to gridding the gradient data.

The Hardwick method is advantageous in that it can be completed in one step as part of the bidirectional gridding process, although the leveling requirements for the gradients may be more stringent prior to gridding. The Nelson method takes several steps (i.e., gridding of the gradients, regional correction, and possibly automated trend enforcement). The minimum-curvature gridding version is more computationally intensive than the bidirectional version. Regardless of the method used, the effort to apply gradient enhancement of the total magnetic field is minimal, relative to the overall costs of a survey.

Comparison of the total magnetic field measured on the control lines with the values interpolated between the traverse lines is a good test of any gridding method (Hardwick, 2004). The gridded data were extracted back to a profile database containing the control line data. Both gradient-enhanced gridding techniques demonstrated much improved location of anomaly peaks and rendering of anomaly shapes as compared to the standard interpolation methods. They did not fully recover the anomaly amplitudes where the peaks were situated midway between traverse lines. The Hardwick method was superior in matching amplitudes, although the Nelson method that incorporated trended gridding came close.

Conclusions and future developments. It is clear from the examples presented here that incorporation of the measured horizontal gradient(s) in preparation of gridded total magnetic field improves the accuracy and resolution of the product. There are some issues with noise effects introduced by each approach, but the improvement in anomaly continuity and shape makes their employment worthwhile.

The efforts to process the profile and gridded gradient data are not limited to gradient-enhanced gridding of the total magnetic field. The gradients are used in a number of transforms (e.g., analytic signal, tilt derivative), interpretive methods (e.g., source-parameter imaging, Euler deconvolution, source-edge detection) and modeling. High-quality gradient data contribute to all facets of the interpretation process.

The current techniques can be further improved by:

- Addressing the noise introduced by the gradient-enhancement methods (e.g., level problems, tearing, clipping) and processing the data to minimize these effects
- Measuring and correcting for aircraft (or bird) orientation, thereby removing the geometric effects of the pitch, roll, and yaw from the measured gradients

- Utilizing the measured vertical gradient as well as the horizontal gradients to compute the total magnetic field on a smooth drape surface, thereby minimizing the effect of height differences between and along lines

The use of a magnetic gradiometer system adds to the survey cost relative to a single sensor. The additional magnetometers increase the chances of downtime due to equipment failure. Additional time is required for magnetometer compensation and data processing. These issues are more than offset by the advantages of including the measured gradients in the data processing and interpretation streams. The improved accuracy and resolution of the magnetic data offer the opportunity to increase the line spacing should cost be an issue. The elimination of tie lines is not advocated, but their spacing may be increased due to the ease of leveling the gradient data. Similarly, use of the gradient data minimizes the problem of diurnal monitoring at significant distance from a survey area. Two wingtip-mounted magnetometers are sufficient to measure the total magnetic field and the two horizontal gradients, assuming that the longitudinal gradient is computed by time differencing. However, the wingtip sensors suffer from more motion and vibration noise than a conventional tail stinger sensor, so a three-sensor system is optimal for measuring the horizontal gradients. A fourth sensor mounted on the tail assembly is preferable for measurement of the vertical gradient, rather than vertically offsetting a single tail sensor and deconvolving the three gradients.

Suggested reading. *Kapuskasing-Chapleau Aeromagnetic Survey, Magnetic Data, Ontario Geological Survey, Geophysical Data Set 1040* (Geological Survey of Canada, 2001). "Gradient-enhanced total field gridding" by Hardwick (1999 *SEG Expanded Abstracts*). "Two methods of gradient-enhanced gridding—A discussion" by Hardwick (2004 *SEG Expanded Abstracts, Workshop on Magnetic Gradiometry*). "Practicalities, pitfalls and new developments in airborne magnetic gradiometry" by Hogg (Annual Meeting of the Prospectors & Developers Association of Canada, 2004). "Measured is better" by McMullan and McLellan (In *Proceedings of Exploration 97: Fourth Decennial International Conference on Mineral Exploration*, 1997). "Leveling total-field aeromagnetic data with measured horizontal gradients (short note)" by Nelson (GEOPHYSICS, 1994). *Bedrock Geology of Ontario, ERLIS Data Set 6* (Ontario Geological Survey, 2001). "Gridding with continuous curvature splines in tension" by Smith and Wessel (GEOPHYSICS, 1990). **TJE**

Corresponding author: stephen.reford@pgwv.on.ca